# A Generalized Critical Flow Model for Nonideal Gases

**J. C. Leung, M. Epstein**
Fauske & Associates, Inc.
Burr Ridge, IL 60521

This paper presents a generalized formulation for evaluating the critical flow rate of a nonideal gas characterized by the Redlich-Kwong (R-K) equation of state (EOS). The case of interest here is one-dimensional isentropic flow in a frictionless nozzle. The solutions for ideal gases are well known and can be found in standard fluid flow references. However, no solution for nonideal gases appears in these sources. An earlier rigorous analysis of critical flow of a van der Waals gas was presented by Tsien (1946). The most comprehensive treatment of nonideal critical flow to date has been due to Johnson (1964, 1965, 1968, 1970, 1971, 1974). His theoretical work resulted in a detailed tabulation of critical flow properties for various common gases for a wide range of thermodynamic conditions. A separate virial-type EOS involving anywhere from seven to 15 parameters was developed for each gas that he considered, and no generalized solution was presented. The present study seeks a generalized treatment in terms of reduced thermodynamic properties. The main focus of this paper is, therefore, to present for the first time generalized plots in a form most engineers would prefer and accurate enough for practical applications. The R-K EOS was favored due to its wide use in practice and its simple two-parameter form. In agreement with previous work by Duxbury (1979), various modifications to the ideal gas flow equations involving the use of the compressibility factor $Z$ were found to be inaccurate when $Z$ deviates substantially from unity.

## Analytical Formulation

Similar to the ideal gas treatment, the critical mass velocity is found by maximizing

$$G = [2(h_o - h)]^{1/2}/v, \tag{1}$$

subject to the constant entropy constraint

$$S_o - S = 0 \tag{2}$$

Since both $h$ and $S$ are point functions, their integrations are path independent. Thus, referring to Figure 1, one can write

$$h_o - h_1 = (h_o - h_o^{id}) + (h_o^{id} - h_1^{id}) + (h_1^{id} - h_1) \tag{3}$$

$$S_o - S_1 = (S_o - S_o^{id}) + (S_o^{id} - S_1^{id}) + (S_1^{id} - S_1) \tag{4}$$

where

$$h_o^{id} - h_1^{id} = \int_{T_1}^{T_o} C_p^{id}\, dT \tag{5}$$

$$S_o^{id} - S_1^{id} = \int_{T_1}^{T_o} \frac{C_p^{id}}{T}\, dT - R \ln \frac{P_o}{P_1} \tag{6}$$

Here the superscript $id$ denotes conditions at zero pressure where ideal gas behavior is obeyed. The remaining terms such as $(h^{id} - h)$ and $(S^{id} - S)$ relate to the departure from ideality at constant temperature. From thermodynamic relationships (for example, Walas, 1985) we can write

$$h^{id} - h = RT - Pv + \int_{\infty}^{v} \left[P - T\left(\frac{\partial P}{\partial T}\right)_v\right] dv \tag{7}$$

$$S^{id} - S = -R \ln Z + \int_{\infty}^{v} \left[\frac{R}{v} - \left(\frac{\partial P}{\partial T}\right)_v\right] dv \tag{8}$$

These forms are most convenient for the pressure-explicit EOS and for the R-K EOS become,

$$h^{id} - h = RT\left[1 - Z + \frac{1.5a}{bRT^{1.5}} \ln\left(1 + \frac{b}{v}\right)\right] \tag{9}$$

$$S^{id} - S = -R\left\{\ln\left[Z\left(1 - \frac{b}{v}\right)\right] - \frac{a}{2bRT^{1.5}} \ln\left(1 + \frac{b}{v}\right)\right\} \tag{10}$$

where $a$ and $b$ are the familiar R-K gas constants, namely

$$a = 0.42748\, R^2\, T_c^{2.5}/P_c;\ b = 0.08664\, RT_c/P_c. \tag{11}$$

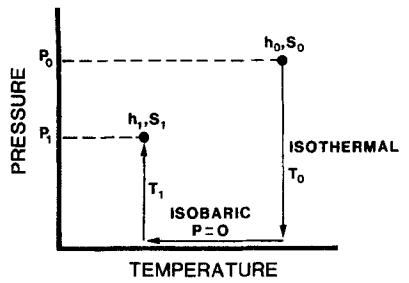


**Figure 1. Thermodynamic paths between point functions.**

We shall now make the usual assumption of a constant $C_p^{id}$ as in the normal treatment of an ideal gas. In doing so, Eqs. 5 and 6 can be readily integrated. Note that if $C_p^{id}$ is represented by a second-order polynomial in $T$, these integrations can be carried out but the resulting expressions for Eqs. 1 and 2 will not permit the degree of simplicity given by the constant $C_p^{id}$ form. Moreover, the present model will be seen to correlate both experimental data and the results from a more elaborate numerical procedure remarkably well.

Upon substitution of Eqs. 6 and 10 into Eq. 2, the following isentropic expansion law between the stagnation and throat conditions is obtained:

$$\frac{T_{rt}}{T_{ro}} = \left[\frac{v_{ro} - \beta}{v_{rt} - \beta}\right]^{\gamma-1} \left[\frac{\left(1 + \frac{\beta}{v_{rt}}\right)^{T_{rt}^{-1.5}}}{\left(1 + \frac{\beta}{v_{ro}}\right)^{T_{ro}^{-1.5}}}\right]^{c_1/2c_2(\gamma-1)} \tag{12}$$

where $\beta = c_2/Z_c$, $c_1 = 0.42748$, $c_2 = 0.08664$ (Eq. 11), and $Z_c = 0.333$. The subscript $r$ pertains to the so-called reduced properties which are normalized by their values at the critical state. Here $\gamma$ is the "ideal" specific heat ratio at *zero pressure*, i.e., $\gamma = C_p^{id}/(C_p^{id} - R)$. Equation 12 is reduced to the ideal gas law form in the limit $c_1 = c_2 = 0$. Identifying state point 1 in Eq. 3 with the throat condition, the normalized mass velocity expression follows from Eqs. 1, 3, 5, and 9,

$$\frac{G}{\sqrt{P_c/(Z_c v_c)}} = \left\{2\left[\frac{1}{\gamma - 1}(T_{ro} - T_{rt}) + Z_o T_{ro} - Z_t T_{rt}\right] + \frac{3c_1}{c_2} \ln \frac{\left(1 + \frac{\beta}{v_{rt}}\right)^{T_{rt}^{-0.5}}}{\left(1 + \frac{\beta}{v_{ro}}\right)^{T_{ro}^{-0.5}}}\right\}^{1/2} v_{rt} \tag{13}$$

Thus the critical flow calculation reduces to one of maximizing Eq. 13 with respect to $v_{rt}$ while simultaneously solving Eq. 12 for $T_{rt}$.

## Results

The results are presented in Figure 2 in terms of the ratio $G/G^{id}$ vs. the reduced stagnation pressure for a nonideal gas with $\gamma = 1.4$. Here $G^{id}$, the ideal-gas "critical" mass velocity, is given

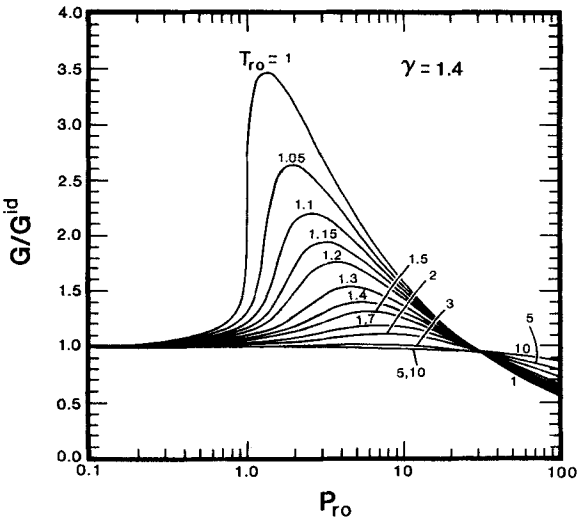


**Figure 2. Generalized chart for $\gamma = 1.4$.**

in the normalized form as

$$\frac{G^{id}}{\sqrt{P_c/(Z_c v_c)}} = Z_c P_{ro}\left[\frac{\gamma}{T_{ro}}\left(\frac{2}{\gamma + 1}\right)^{(\gamma+1)/(\gamma-1)}\right]^{1/2} \tag{14}$$

Our findings indicate that the maximum deviation from the

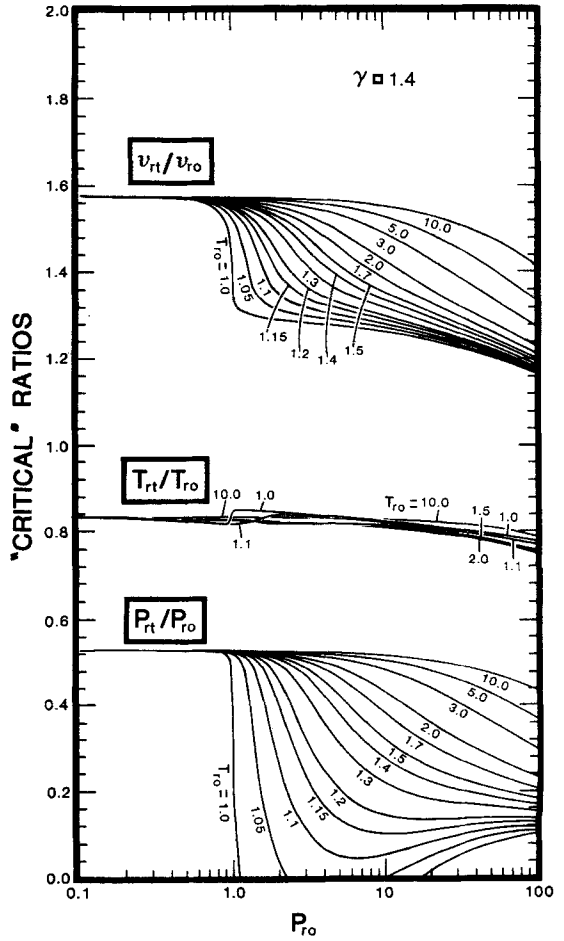


**Figure 3. "Critical" ratios for $\gamma = 1.4$.**

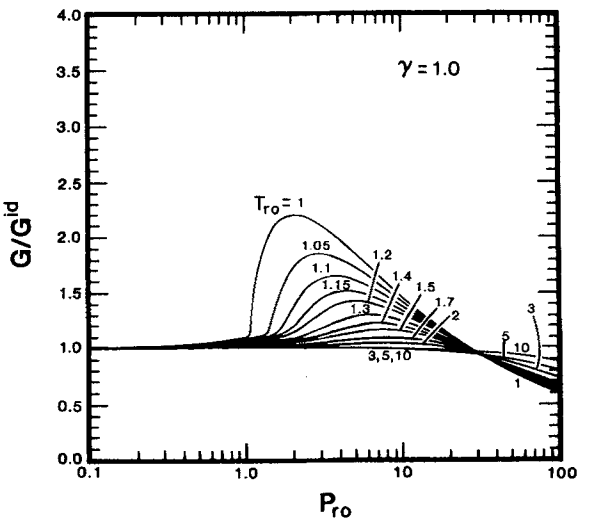


**Figure 4. Generalized chart for $\gamma = 1.0$.**

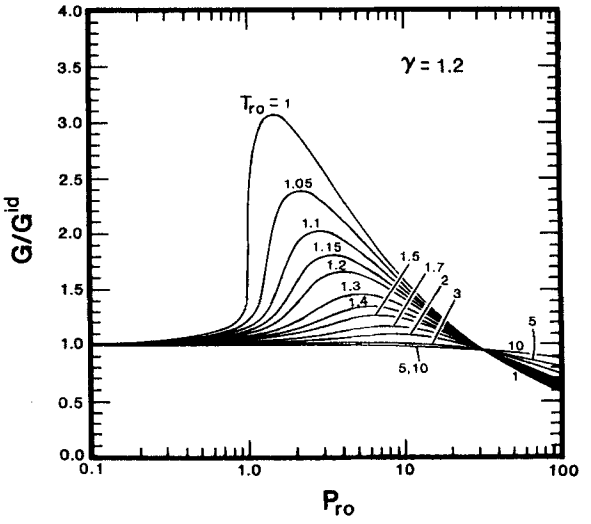


**Figure 5. Generalized chart for $\gamma = 1.2$.**

ideal gas flow rate occurs at $T_{ro} = 1.0$ and $P_{ro} = 1.4$. As expected, deviation from ideal gas flow diminishes as $T_{ro}$ increases. At $T_{ro}$ of 5 and above, the ideal gas flow rate is closely approached.

The reduced "critical" specific volume, temperature, and pressure at the choked (throat) location are presented as ratios with respect to the reduced stagnation quantities in Figure 3, again for a $\gamma$ of 1.4. Unlike specific volume ratio and pressure ratio, the temperature ratio is rather insensitive to variations in the stagnation conditions. It is noted that most of the deviation from ideal behavior (as represented by the values at $P_{ro} \sim 0.1$) occurs near the thermodynamic critical pressure ($P_{ro} = 1$) and critical temperature ($T_{ro} = 1.0$). For reduced stagnation temperatures ($T_{ro}$) of 1.0 and 1.05, the pressure at the choked point becomes negative in certain regions, as can be seen from Figure 3. These nonphysical states correspond to two-phase choked conditions which were not treated in this study.

Similar $G/G^{id}$ charts are shown in Figures 4, 5, and 6 for specific heat ratios of 1.0, 1.2, and 1.67. These charts together with Figure 2 indicate, in the $P_{ro}$ range 1–10, a progressive flow augmentation relative to the ideal gas case as $\gamma$ increases. However, at $P_{ro}$ over 20, these charts actually show a gradual decrease in flow relative to the ideal gas value with increasing $P_{ro}$.

## Comparison of Model and Literature Data

Comparison is made between the present model and the very detailed numerical calculations for selected gases by Johnson (1965, 1968, 1972) in the reduced pressure range of 0.1 to 10. These gases include argon, hydrogen, air, nitrogen, oxygen, water, and methane. As noted earlier, Johnson's predictions were based on very complex (virial type) EOS specifically developed for individual gases. Figure 7 shows that the proposed generalized model which is based on the two-parameter R-K EOS is in good agreement with Johnson's numerical data. The small discrepancies are likely due to the use of different EOS. It is apparent from Figure 7 that Johnson's results are in support of the generalized charts presented here.

Only limited experimental data are found in the open literature at high pressures such that nonideality is important. Hendricks (1974) presented experimental critical nozzle data for parahydrogen at two widely differed stagnation conditions. For the high temperature region ($T_{ro}$ ranging from 8.0 to 8.7), the measured data are in good agreement with the ideal gas prediction as shown in Figure 8, for $P_{ro}$ ranging from 1.5 to 4.0. Indeed at these high reduced temperatures the present model, Figure 2, predicts negligible deviation from the ideal gas model. However, for the lower temperature region ($T_{ro}$ ranging from 1.1 to 1.2), the ideal gas model significantly underpredicts the measured critical flow rates while the present nonideal gas model yields closer agreement (to within 10%) as shown in Figure 8.

Finally, Figure 9 presents a plot of $G/G^{id}$ vs. the stagnation compressibility factor $Z_o$ at various reduced temperatures. For $Z_o$ less than unity where flow augmentation is most pronounced, we find that the ratio $G/G^{id}$, and hence the flow rate, cannot be uniquely determined by $Z_o$ alone. This would dispute any method that attempts to correct the ideal gas model by some simple algebraic modification involving the compressibility factor.

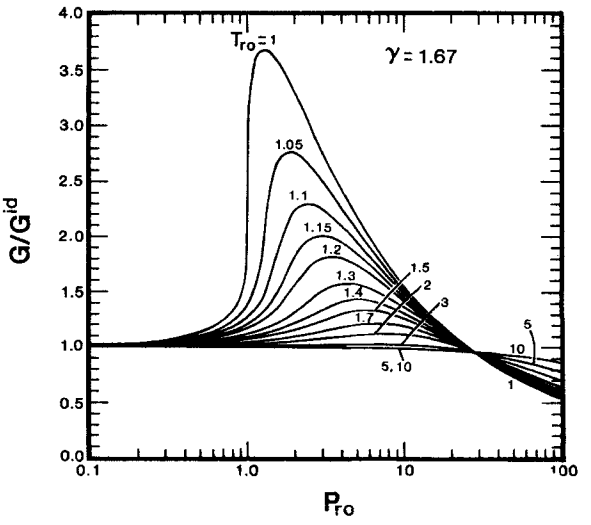


**Figure 6. Generalized chart for $\gamma = 1.67$.**

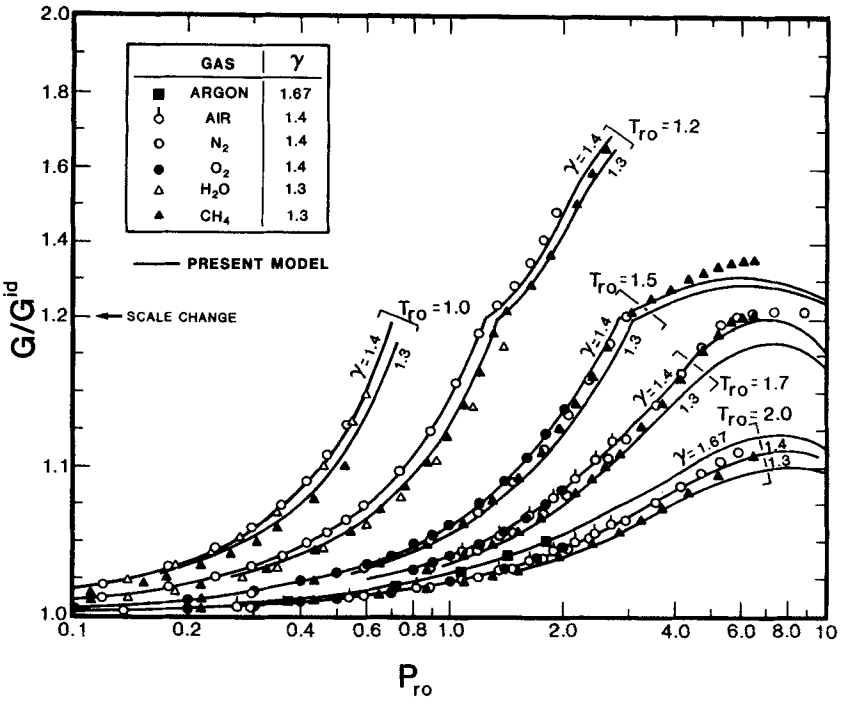


**Figure 7. Comparison between present model and Johnson's data.**

## Conclusions

By adopting the R-K EOS, generalized charts have been obtained for the prediction of the critical flow rate of a nonideal gas. The charts, which focus attention on a minimum number of basic dimensionless, reduced thermodynamic properties clearly display the conditions under which large departures from the ideal flow rate can be expected. While the R-K EOS (and other cubic EOS) are known to be of limited accuracy near the critical region, we have shown by comparison with both experimental data and critical flow rates predicted with more complete but less general EOS that the charts presented here are accurate enough for most engineering applications. If it is felt that additional accuracy is required in certain applications, the particular EOS specially developed for the gas of interest should be used, although the differences between the critical flow predictions based on the R-K EOS and those obtained with such a complex EOS are likely to be no greater than the uncertainty in critical flow measurements.

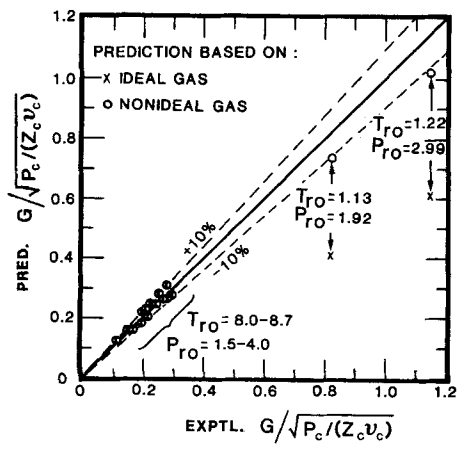


**Figure 8. Comparison of model with Hendrick's experimental data.**

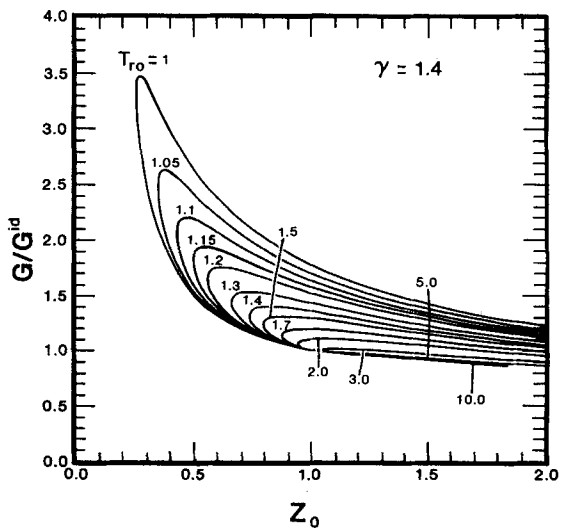


**Figure 9. Variation of $G/G^{id}$ vs. stagnation compressibility.**

## Acknowledgments

The authors are indebted to R. C. Hendricks (NASA Lewis Research Center) for supplying key references and to G. M. Hauser (Fauske & Associates, Inc.) for carrying out initial calculations.

## Notation

$a, b$ = parameters in R-K EOS
$c_1, c_2$ = constants in R-K EOS, Eq. 11
$C_p$ = constant pressure specific heat

$h$ = specific enthalpy
$G$ = mass velocity
$P$ = pressure
$R$ = gas law constant
$S$ = specific entropy
$T$ = temperature
$v$ = specific volume
$Z$ = compressibility factor

### Greek letters

$\beta$ = parameter $c_2/Z_c$
$\gamma$ = zero-pressure specific heat ratio

### Subscripts

$c$ = thermodynamic critical point
$o$ = stagnation condition
$r$ = thermodynamic reduced property
$t$ = throat condition

### Superscript

$id$ = ideal gas

## Literature Cited


Duxbury, H. A., "Relief Line Sizing for Gases—(Two Parts)," *The Chem. Engr.*, 783, 851 (Nov., 1979).

Hendricks, R. C., "Normalized Parameters for the Critical Flow Rate of Simple Fluids Through Nozzles," Paper J10, Int. Cryog. Eng. Conf., ed. K. Mendelssohn, IPC Science and Technology Press, 278 (1974).

Johnson, R. C., "Calculations of Real-Gas Effects in Flow Through Critical-Flow Nozzles," *J. of Basic Eng. Trans. ASME*, **86**, 519 (1964).

———, "Calculations of the Flow of Natural Gas Through Critical Flow Nozzles," *J. of Basic Eng. Trans. ASME*, **92**, 580 (1970).

———, "Real-Gas Effects in Flow Metering," in Flow—Its Measurement and Control in Science and Industry, Volume I, R. B. Dowdell editor-in-chief, pp. 269–278 (1974).

———, "Real-Gas Effects in Critical-Flow-Through Nozzles and Tabulated Thermodynamic Properties," NASA TN D-2565 (1965).

———, "Real-Gas Effects in Critical Flow Through Nozzles and Thermodynamic Properties of Nitrogen and Helium at Pressures to 300 $\times$ $10^5$ N/m$^2$ (Approx. 300 atm)," NASA SP-3046 (1968).

———, "Tables of Critical-Flow Functions and Thermodynamic Properties for Methane and Computational Procedures for Both Methane and Natural Gas," NASA SP-3074 (1972).

———, "A Set of Fortran IV Routines Used to Calculate the Mass Flow Rate of Natural Gas Through Nozzles," NASA TM X-2240 (1971).

Tsien, H. S., "One-Dimensional Flows of a Gas Characterized by van der Waals Equation of State," *J. Math and Phys.*, **25**, 301 (1946).

Walas, S. M., *Phase Equilibria in Chemical Engineering*, Butterworth, London, Ch. 11 (1985).



*Manuscript received Dec. 29, 1987, and revision received May 6, 1988.*